Random Vibration and Acoustic Analysis Using ARI RANDOM, a NASTRAN Post Processor

R.D. Galletly

R.J. Wagner

G.J. Wang

J.W. Zins

Jet Propulsion Laboratory,
California Institute of Technology,
Padadena, California

ABSTRACT

This presentation describes the theory and application of ARI RANDOM. The results of three analytical studies are reviewed. These are:

- o Wide Field Planetary Camera random vibration and acoustic analysis
- o Galileo Spacecraft acoustic analysis
- o All Source Analysis System shelter transportation vibration analysis

INTRODUCTION

Two major structural test programs of space hardware were recently completed at the Jet Propulsion Laboratory (JPL).

They were the Wide Field Planetary Camera (WFPC) a scientific instrument mounted on the Space Telescope and the Galileo (GLL) spacecraft designed for the scientific exploration of Jupiter.

These two test programs placed a high emphasis on the pretest planning, analytical predictions, and instrumentation. This was necessitated in the WFPC random and acoustic tests because the test was performed to protoflight levels on the flight hardware and there was no precursor structural test article. This placed a very high emphasis on the pretest predictions in order to protect the flight structure from an overtest. Also, the analysis provided an early indication of potential structural problems.

The GLL test program involved a critical acoustic test schedule. The acoustic test was immediately following and preceding other structural tests and was completed in two days. Therefore pretest analysis was needed to assess the data between levels of testing in a timely manner.

JPL is also involved in the preliminary design of the All Source Analysis System (ASAS). A typical shelter, a 20' ISO Intel Data Processing Shelter (IDPS) with 45" work stations, was modeled and analyzed to determine the response of equipment to severe off-road transportation environments. This was done in order to size the structural elements and study the feasibility of utilizing commercial electronic equipment in this application.

NASTRAN finite element models were generated and ARI RANDOM was selected as the analytical tool for these efforts. The method of analysis and a summary of results for these three (3) studies are reported in this document.

ANALYSIS

Summary of ARI RANDOM

ARI RANDOM is a user oriented, versatile application program used to analyze the response of multi-degree-of-freedom linear elastic structural models subjected to stationary random dynamic loading. The normal mode method is employed. RANDOM computes root mean squared (RMS) grid point displacements, velocities and accelerations. Response power spectral density (PSD) curves

are generated for selected grid degrees of freedom. The RMS loads and stresses may be computed for user selected NASTRAN element types. The input forcing power spectra may be defined in general terms by the shape of the spectrum and type of spatial correlation. The responses which are generated from the base acceleration can be computed as either relative or absolute values. A flow chart for RANDOM is shown in Figure 1. A complete description of the RANDOM program can be found in Reference 1. The equations of motion are described in Appendix A.

RANDOM Input/Output Characteristics

Inputs to the program include NASTRAN generated modes shapes, frequencies, selected element modal loads and stresses from tapes (or disc). User-supplied data describing the types and characteristics of random excitation are required. The excitation may include combinations of mechanical forces, acoustic pressure fields or base excitations that have various PSD shapes and spatial correlations.

Outputs from the program include RMS grid point displacements, velocities and accelerations and response PSD curves for selected degrees of freedom. Base acceleration response outputs may be relative or absolute values.

The output is presented in the form of computer printouts and, if requested, PSD plots of selected degrees of freedom.

Summary of Procedure

1. Examine the RANDOM program dimensional capability for permissible program parameters (e.g. number of NODES, MODES, etc.) The program dimensional capabilities are shown in Table 1.

2. Create the structural model using finite elements.

3. Input the structural model to the NASTRAN program to obtain a suitable number of mode shapes and frequencies (eigenvectors and eigenvalues).

4. Save the file containing the data generated in step 3 for subsequent input to RANDOM.

5. Prepare the RANDOM Input Cards.

6. Prepare the Control Cards. Cards are required to initiate the job; read the tape containing mode shapes, frequencies, element load and stress. Copy this information to a file for RANDOM and Execute RANDOM. If desired, cards must be provided to process plot outputs.

Random Vibration Analysis

The random vibration analysis performed predicted the response of mathematical models subjected to base excitation. The mathematical models simulated the primary structural elements and mass distribution of system under investigation. The base excitation was described by a power spectral density of acceleration and the motion of all base support points was fully correlated with other base support points.

Normal modes, frequencies and damping were selected in the range of interest to determine the response of major structural elements and components.

Acoustic Analysis

Similar to the random vibration analysis, the acoustic analysis utilized the mathematical model of the system under investigation. The acoustic excitation was defined by a sound pressure level (SPL). The SPL was described in 1/3 octave bands with center frequencies encompassing the frequency range of the excitation. The SPL was applied over the exterior surface areas of the system model. The exterior surface areas were divided into convenient sections around grid points and the SPL integrated over these area sections providing an equivalent point force applied at the grid point. The applied force acted normal to the area section. The resulting set of applied point forces simulated the effect of the acoustic excitation. All point forces were fully correlated with each other. The frequency range of interest for the response of the primary structure and major components was below 300 Hz.

DESCRIPTION OF SYSTEMS ANALYSED

The Wide Field Planetary Camera is a large 272 kg (600 lbs) scientific instrument mounted on the Space Telescope. The WFPC was designed, built and tested at JPL. The Space Telescope will be launched on the Space Transportation System (STS) in 1986. The WFPC is shown in Figure 2.

The Galileo is a spacecraft designed for the scientific exploration of Jupiter. This 2,500 kg (5,500 lb) spacecraft (S/C) was also designed, built and tested at JPL and will be launched in 1986 as a dedicated STS payload. The GLL is shown in Figure 3.

The All Source Analysis System 20' ISO Intel Data Processing Shelter with 45" work stations is a mobile ground unit used for field communications in military maneuvers. The shelter weighs 6 to 7 tons when fully loaded and will be transported on a 10 ton HEMTT truck. An ISO 20' is shown in Figure 4.

WFPC Random Vibration Analysis

The WFPC random vibration analysis utilized a NASTRAN finite element model. The model parameters are shown in Table 2. The number of normal modes used was 25 and the modal damping coefficient was 1% of critical for all modes. The base excitation magnitude is shown in Table 3. The direction of excitation was in the axial direction of the radiator (VI) as shown in Figure 1. A plot of the undeformed finite element model is shown in Figure 5.

WFPC Acoustic Analysis

The WFPC acoustic analysis also utilized a NASTRAN finite element model whose parameters are shown in Table 2. Note that the model was modified by replacing CSHEAR elements with CQUAD4 elements to ease the application of the sound pressure over the external surface areas of the WFPC assembly. The number of normal modes used was 25 and the modal damping coefficient was 1% of critical for all modes. The sound pressure level intensity and frequency distribution is shown in Table 4. The WFPC model was divided into 44 area zones each producing a single point force simulating the local effect of the sound pressure.

GLL Acoustic Analysis

The GLL acoustic analysis utilized a NASTRAN finite element model whose parameters are given in Table 2. The number of normal modes used was 100, the maximum that can be presently used in ARI RANDOM. The modal damping coefficient was 1% of critical for all modes. The sound pressure level intensity and frequency distribution is shown in Table 5. The GLL model was divided into 90 area zones each producing a single point force simulating the local effect of the sound pressure. A plot of the undeformed finite element model is shown in Figure 6.

ASAS Random Vibration Analysis

The IDPS transportation random vibration response analysis utilized a detailed NASTRAN finite element computer model. The various components of the model are shown in Figure 7. The shrink option was employed on Figure 7 for clarity in presentation of these components. The walls, roof, floor and ends of the shelter are of foam and beam construction with aluminum facesheets. The racks are fully integrated with the basic shelter. The equipment was modeled to have natural frequencies between 15 and 50 Hz. Table 2 presents the model characteristics as used for the transportation response predictions. Modes up to 100 Hz were retained with modal damping 2% of critical being used for all modes. Base input Power Spectral Densities are shown in Figures 8 through 10 for each of the translational directions. They are taken from Military Standard 810D, applied simultaneously, and are assumed to be fully correlated. A tabular listing of the breakpoints is also presented with each figure. The weight of the shelter used in the analysis was 12,736 pounds.

RESULTS

The results of the previous described studies are summarized in the following sections. These results include RMS grid point accelerations and strains. Response PSD plots for selected degrees of freedom are also shown.

WFPC Response Summary

Table 6 reveals a summary of the response predictions for the WFPC random vibration test. Both RMS accelerations and strains are shown. Table 7 provides a summary of the response predictions for the WFPC acoustic test. Again, both RMS accelerations and strains are shown. Figures 11 through 12 are representative response PSD plots. Figure 2 can be used as an aid to identify the prediction location.

GLL Response Summary

Table 8 lists a summary of the response predictions for the GLL acoustic test. RMS accelerations at various locations and indicated directions are shown. Figures 13 through 15 reveal typical PSD Plots. Figure 3 is provided to show the general arrangement of the GLL spacecraft.

ASAS Response Summary

Table 9 provides a summary of predicted responses for work station equipment in an ISO 20' shelter during off-road transportation. Similarly, Table 10 shows the racked equipment response summary. RMS accelerations are given in these tables. Figures 16 through 18 are selected response PSD plots. Figure 4 shows the general layout of an ISO 20' with description to locate the response region and direction.

DISCUSSION/CONCLUSIONS

ARI RANDOM interfaces conveniently with NASTRAN generated data. RANDOM has proven to be versatile and user oriented. It should be stated that in its present version RANDOM solutions are only valid where normal modes from the NASTRAN generated finite element model are representative of the actual system under investigation. This limitation requires the analyst to review the normal modes carefully, particularly at higher frequencies, and reject unsatisfactory modes. Care must also be taken in selection of the cross-mode coupling parameter and the frequency bounds of the integration procedure in order to establish a balance between solution accuracy and cost savings.

ARI RANDOM has been successfully used as a planning tool for vibro-acoustic testing. This application was utilized for the WFPC and GLL and is documented in Reference 2. Further, RANDOM was used as an aid to size structural elements and predict equipment and workstation response levels.

Future improvements for ARI RANDOM that should be considered include:

- o The addition of a statistical energy method to estimate response at higher frequency.
- o Tabulating the RMS response values as a function of frequency to support test data analysis.
- o A technique to modify a free acoustic field for the presence of a payload.
- o A summary of maximum/minimum response RMS predictions to determine peak values and associated locations.

ACKNOWLEDGEMENT

The work described in this paper was carried out by the Jet Propulsion Laboratory, California Insittute of Technology. The authors additionally acknowledge the support of J. A. Clements of Applied Research Incorporated; M. D. Lamers of Measurement Analysis Corporation; D.H. Rodgers, R.F. Tillman, and W.J. Carley of the Jet Propulsion Laboratory.

REFERENCES

1. ARI RANDOM NASTRAN Post Processor User's Guide, Revision 1, September 1982.

2. Galletly, R.D., Tillman, R.F., "A Comparison of the Analytical Predictions and Results from Random Vibration and Acoustic Tests of the Wide Field Palnetary Camera and the Galileo Spacecraft", Shuttle Payload Dynamic Environments and Loads Prediction Workshop, January, 1984.

Table 1

RANDOM PROGRAM DIMENSIONAL CAPABILITIES

Number of Grid Points	1666
Grid Point Number	999999
Number of Modes	100
Number of Forcing Function PSD's	10
Number of Grid Points for printing and Plotting PSD responses	9996
Number of Extra Frequency points	800
Number of frequency points including extra frequency points from above	3000

Table 2

FINITE ELEMENT MODEL CHARACTERISTICS

Model Parameter	WFPC Random Vib. Analysis	MODEL Acoustic Analysis	GLL Acoustic Analysis	ASAS Transportation Analysis
Number of Grid Points	698	698	1651	514
Number of Static Degrees of Freedom (DOF)	3822	3822	9906	2994
Number of Finite Elements	(1071)	(1059)	(2777)	(1387)
CBAR	341	341	1542	641
CBEAM	2	2	0	0
CELAS2	6	6	3	0
CONROD	0	0	119	0
CQUAD4	448	494	645	487
CROD	12	0	98	0
CSHEAR	46	0	132	0
CTR1A2	0	0	232	0
CTR1A3	216	216	6	258
Number of Mass Degrees of Freedom	2090*	2090*	2169*	1521*
Number of Dynamic Degrees of Freedom (ASET)	161	161	162	375
Number of Modes Retained - Analysis	25	25	100	67
Frequency Upper Bound - Analysis	213 Hz	222 Hz	140.0 Hz	99 Hz

*Includes mass DOF generated through density option in NASTRAN.

Table 3

WFPC RANDOM VIBRATION TEST LEVEL

Frequency (Hz)	Test Level (Protoflight)
20 - 80	+5 dB/Octave
80 - 300	.02 g^2/Hz
300-2000	-9 dB/Octave
Overall	2.85 grms

Table 4

WFPC 1/3 OCTAVE BAND ACOUSTIC LEVELS AND TOLERANCES

Sound Pressure Level (dB) Ref. 2 X 10-5 N/m^2

1/3 Octave Band Center Frequency (Hz)	Protoflight	
	Level	Tolerance
31.5	131.5	+6, -12
40	133.5	+5, -12
50	135.5	+5, -9
63	137.0	+4, -8
80	137.0	+4, -7
100	137.0	+3, -6
125	137.5	+3, -5
160	136.5	+3, -4
200	136.0	+3, -3
250	135.0	+3, -3
315	133.5	+3, -3
400	133.0	+3, -3
500	131.5	+3, -3
630	130.5	+3, -3
800	129.0	+3, -3
1000	127.5	+3, -3
1250	126.5	+3, -3
1600	125.5	+3, -3
2000	124.0	+3, -4
2500	122.5	+3, -4
3150	121.5	+3, -5
4000	120.5	+3, -5
5000	119.0	+3, -6
6300	117.5	+3, -6
8000	116.5	+3, -6
10000	115.0	+3, -6
Overall	147.0	+1.5, -1.5

Table 5

GLL 1/3 OCTAVE BAND ACOUSTIC LEVELS AND TOLERANCES

Sound Pressure Level in (dB) Ref. 2x10-5 N/m^2

1/3 Octave Band Center Frequency (Hz)	Protoflight	
	Level	Tolerance
31.5	128	+6, -10
40	133	+5, -9
50	134.5	+5, -9
63	136	+5, -8
80	136.5	+4, -7
100	136.5	+3, -6
125	136	+3, -5
160	137	+3, -4
200	137.5	+3, -3
250	137	+3, -3
315	136	+3, -3
400	135	+3, -3
500	133	+3, -3
630	132	+3, -3
800	130.5	+3, -3
1000	129	+3, -3
1250	128	+3, -3
1600	127	+3, -3
2000	126	+3, -3
2500	125	+4, -3
3150	124	+5, -3
4000	122.5	+6, -3
5000	121	+6, -3
6300	119.5	+7, -3
8000	118	+8, -3
10000	116.5	+9, -3
Overall	147	+1, -1

Table 6

WFPC RANDOM VIBRATION RESPONSE PREDICTIONS

Acceleration (grms)

Number*	Location	Prediction
253-1	Bay 5	4.3
253-2		1.4
253-3		2.9
254-1	Radiator	3.6
254-2	Corner	4.0
254-3		9.3
256-1	Optical Filter	2.1
256-2		3.0
256-3		3.1
257-1	Camera Head	3.3
257-2	Bulkhead	3.1
257-3		2.7
298-1	Housing Rear	2.6
298-2	Corner	1.3
298-3		2.7
303-1	Forward Mech	3.6
303-2	Cover	2.7

Strain Data (rms)

Number	Location	Prediction Full Prediction
280	Optical Bench Forward Strut	325 lb
288	Pick-Off Mirror Arm	134 in-lb
294	Radiator Truss	38 lb

* The direction of response is indicated by the dash number corresponding to V1, V2 and V3 on Figure 2.

Table 7

WFPC ACOUSTIC RESPONSE PREDICTIONS

Acceleration (grms)

Number*	Location	Prediction
253-1	Bay 5	1.6
253-2		1.6
253-3		1.5
254-1	Radiator	3.5
254-2	Corner	3.3
254-3		8.5
256-1	Optical Filter	.8
256-2		2.5
256-3		1.0
257-1	Camera Head	.6
257-2	Bulkhead	.4
257-3		.6
298-1	Housing Rear	1.9
298-2	Corner	1.0
298-3		1.4
303-1	Forward Mech	1.3
303-2	Cover	2.2
		.8

Strain Data (rms)

Number	Location	Prediction Full Prediction
283	Optical Bench Forward Strut	37 lb
285	Optical Bench AFT Strut	33 lb
289	Pick-Off Mirror Arm	20 in-lb
294	Radiator Truss No. 2	61 lb.

* The direction of response is indicated by the dash number corresponding to V1, V2 and V3 on Figure 2.

Table 8

GLL ACOUSTIC RESPONSE PREDICTIONS

Channel* ID	Location	Acceleration (grms) Prediction
1101X	SXA Tip Lat.	3.3
1102Y	SXA Tip Lat.	3.5
1103Z	SXA Tip Vert.	1.1
1107X	SXA C.G. Lat.	5.1
1108Y	SXA C.G. Lat.	5.0
1106Z	SXA C.G. Vert.	1.1
2131X	Bus-Bay 1/8 LCO	0.7
2132Y	Bus-Bay 1/8 LCO	0.7
2133Z	Bus-Bay 1/8 LCO	0.7
271X	Bus-Star Scan Ft	1.1
272Y	Bus-Star Scan Ft	1.5
273Z	Bus-Star Scan Ft	1.0
8102Y	Probe C.G. (Int)	0.4
8103Z	Probe C.G. (Int)	0.4
7001Y	CET RTG NearTruss	1.3
7004Y	CET RTG Md SpanTr	1.3
7005X	CET RTG Near BTM	1.7
733Z	CET RTG End Flange	0.3
524X	Lwr. Sc. Boom Mag	1.8
525Y	Lwr. Sc. Boom Mag	2.5
526Z	Lwr. Sc. Boom Mag	2.4
671X	Scan Platform	0.9
672Y	Sc. Platfm UVS I.F.	1.0
673Z	Sc. Platfm UVS I.F.	0.7
661X	Sc. Platfm PPR I.F.	0.9
662Y	Sc. Platfm PPR I.F.	1.0
663Z	Sc. Platfm PPR I.F.	0.7
531X	PLS/Supt. Truss	2.8
532Y	PLS/Supt. Truss	2.2
533Z	PLS/Supt. Truss	3.6
4401X	RRH Ant/Supt.-Fwd	16.6
4403Z	RRH Ant/Supt.-Fwd	4.1
4405Z	RRH Ant/Supt.-Aft	12.2
4101X	Dspn-Bx-Ant.Side Inbd - Top Cover	1.9
4102Y	" " "	1.4
4103Z	" " "	1.4
371X	Thrust Clus +X side	1.7
372Y	Thrust Clus +X side	2.7
373Z	Thrust Clus +X side	3.0
521X	Sci Room Mag	14.1
522Y	Sci Boom Mag	11.4
523Z	Sci Boom Mag	2.6
801X	Despun Box Btm Cov	1.9
802Y	Despun Box Btm Cov	1.4
803Z	Despun Box Btm Cov	1.4

* The direction of response is X, Y or Z as indicated in the column and in Figure 3.

Table 9

WORK STATION EQUIPMENT RANDOM VIBRATION RESPONSE PREDICTIONS

Acceleration (grms)

Grid	Weight	X	Y	Z	Location
851	80	3.66	2.30	6.91	F1
852	80	4.78	2.38	5.81	"
853	80	4.93	2.39	5.70	"
854	80	3.91	2.36	6.43	"
857	70	5.12	2.92	5.47	F2
858	70	6.06	2.89	4.22	"
859	70	6.25	2.88	4.14	"
860	70	5.66	2.89	5.25	"
863	70	6.41	4.62	5.48	F3
864	70	7.33	4.64	4.15	"
865	70	7.58	4.69	4.05	"
866	70	7.14	4.75	5.24	"
869	55	7.36	5.38	9.13	F4
870	55	8.17	5.36	4.81	"
871	55	8.45*	5.38	4.44	"
872	55	8.20	5.41	8.41	"
855	80	4.53	4.87	9.58	R1
856	80	5.38	4.85	6.68	"
861	70	5.59	5.62	6.62	R2
862	70	6.58	5.61	4.59	"
867	70	6.60	6.69	6.19	R3
868	70	7.69	6.68	4.37	"
873	55	7.38	7.32*	10.13*	R4
874	55	8.40	7.31	5.53	"

Note: R = Roadside
F = Front
1 = Lower Level
2 = Mid Level
3 = Mid Level
4 = Upper Level
* Maximum Value for Direction

Table 10

RACKED EQUIPMENT RANDOM VIBRATION RESPONSE PREDICTIONS

Acceleration (grms)

Grid	Weight	X	Y	Z	Location
755	70	4.32	6.22	10.50	R1
756	160	4.37	6.11	6.45	"
757	160	4.23	5.33	6.92	"
764	60	5.37	6.96	9.45	R2
765	135	5.61	6.86	6.86	"
766	135	5.56	6.18	6.53	"
773	40	6.49	7.51	29.08*	R3
774	90	6.66	7.38	6.28	"
775	90	6.77	6.87	7.40	"
782	30	7.32	7.99	27.65	R4
783	65	7.48	7.84	14.45	"
784	65	7.54	7.42	10.28	"
758	115	4.95	6.01	5.99	C1
759	200	5.29	6.71	6.53	"
760	200	5.42	7.03	6.35	"
761	280	5.56	7.01	7.12	"
762	125	5.16	6.33	6.56	"
763	315	3.21	5.66	7.55	"
767	95	6.45	7.16	5.95	C2
768	175	6.80	7.88	6.19	"
769	175	6.93	8.18	6.10	"
770	240	7.14	8.08	6.81	"
771	105	6.79	7.32	5.21	"
772	270	7.09	6.58	7.26	"
776	65	7.56	7.93	8.61	C3
777	115	7.85	8.53	6.21	"
778	115	7.97	8.79	5.86	"
779	160	8.19	8.67	5.67	C3
780	70	8.00	7.99	7.96	"
781	180	8.43	7.29	5.81	"
785	50	8.37	8.43	6.89	C4
786	85	8.59	8.90	4.92	"
787	85	8.71	9.10*	4.78	"
788	120	8.91	9.01	6.91	"
789	50	8.78	8.43	7.29	"
790	135	9.13*	7.80	5.99	"

Note: R = Roadside
C = Curbside
1 = Lower Level
2 = Mid Level
3 = Mid Level
4 = Upper Level
* Maximum Value for Direction

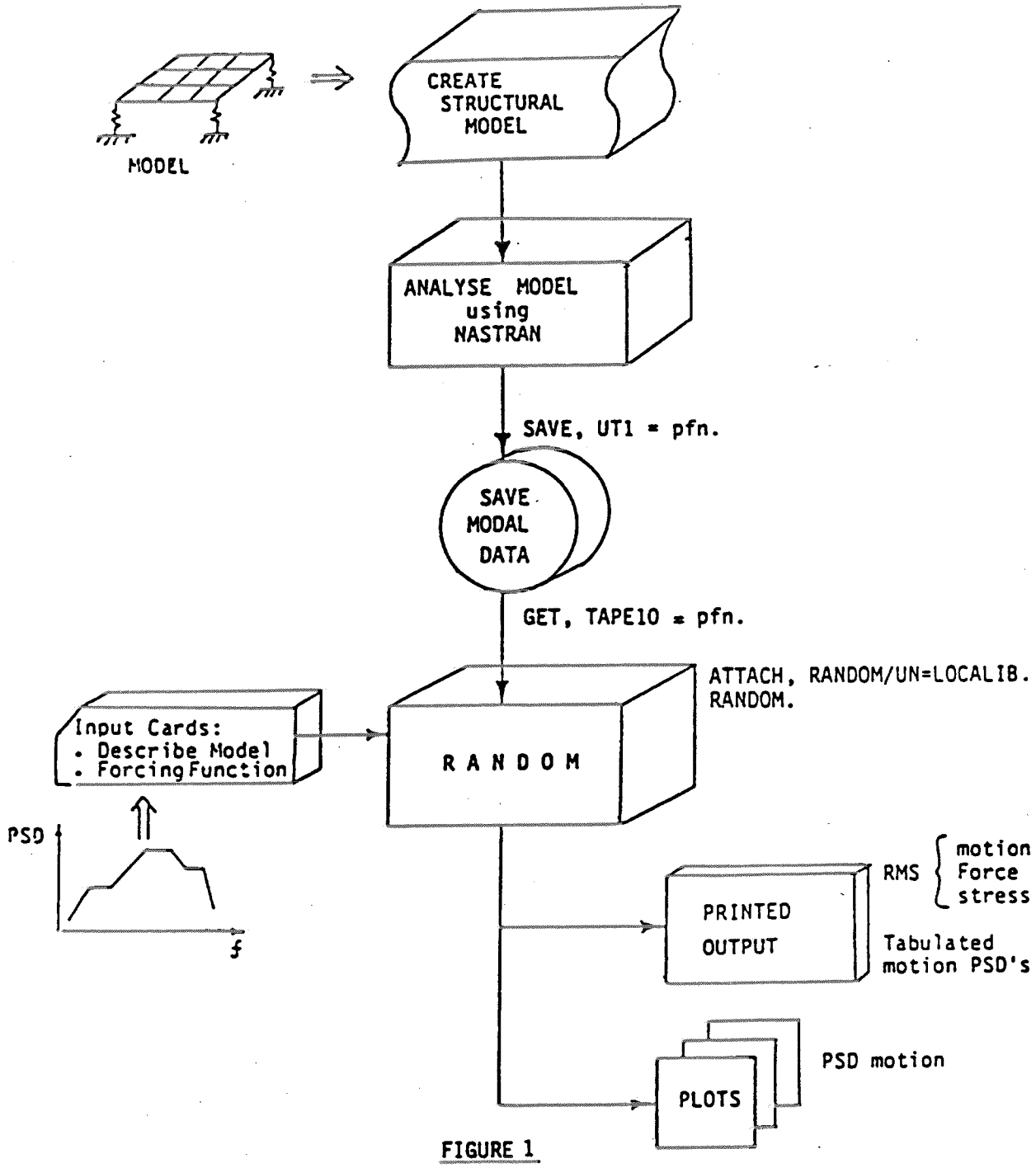

FIGURE 1

ARI RANDOM FLOW CHART

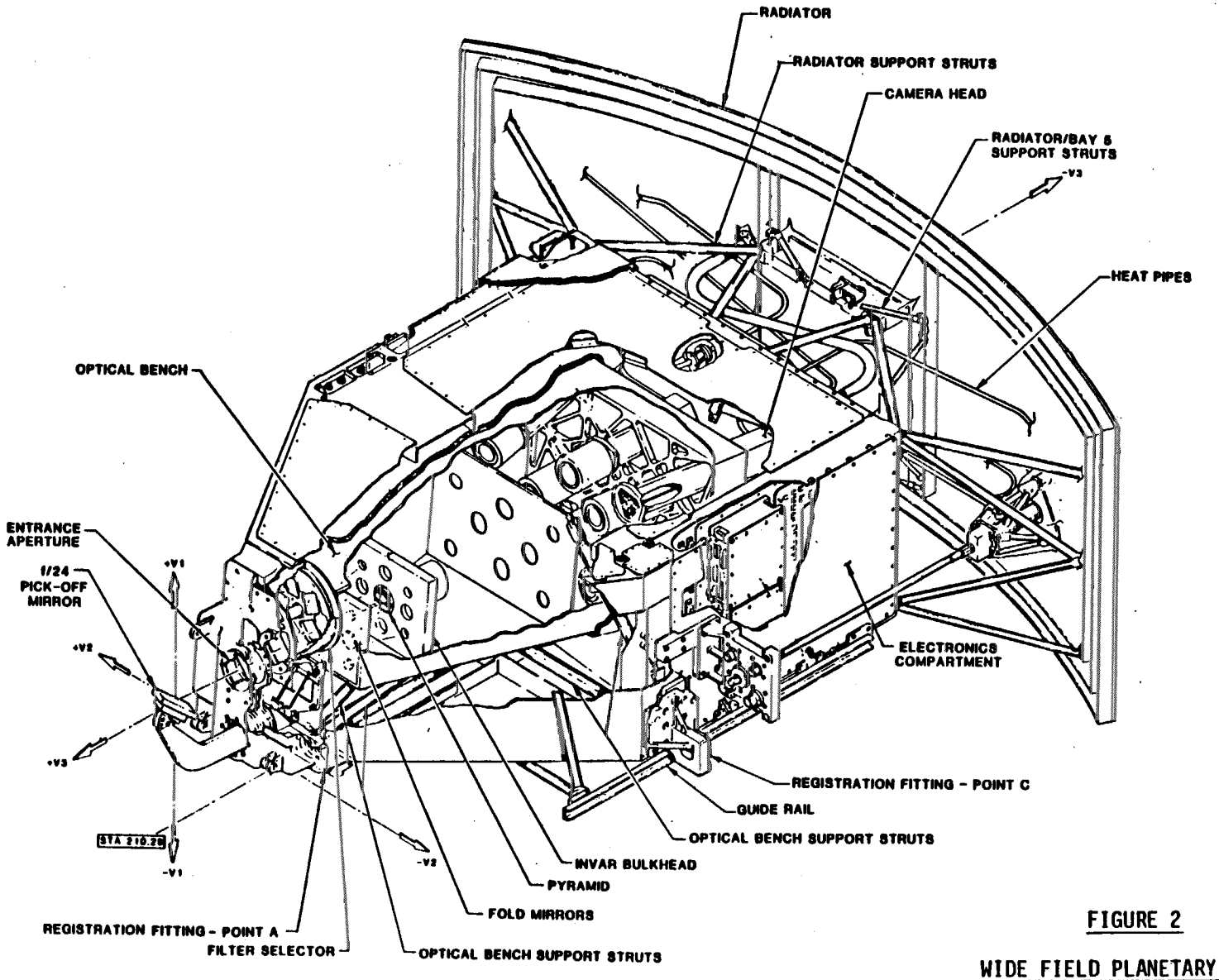

FIGURE 2

WIDE FIELD PLANETARY CAMERA

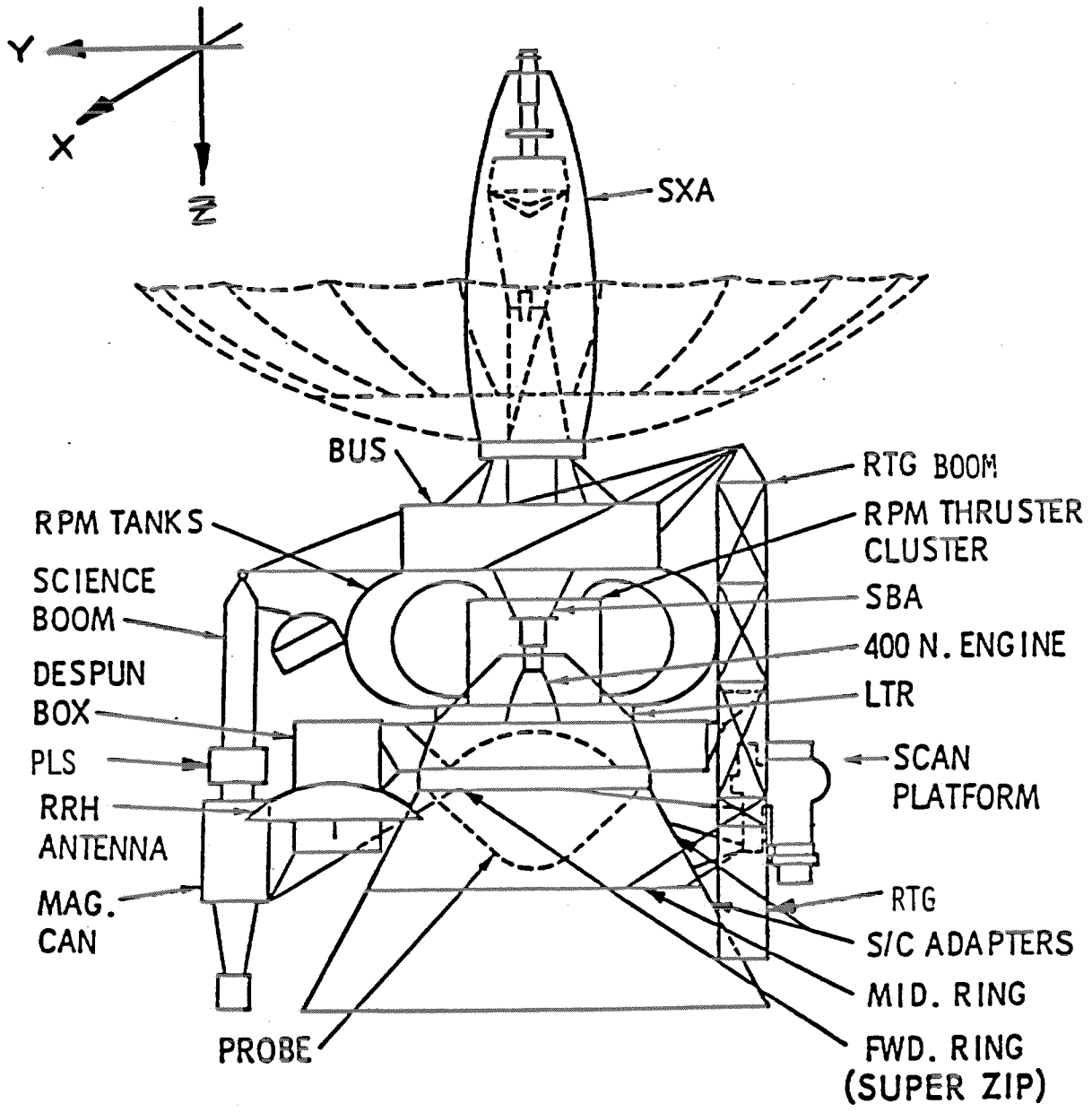

FIGURE 3

GALILEO SPACECRAFT CONFIGURATION

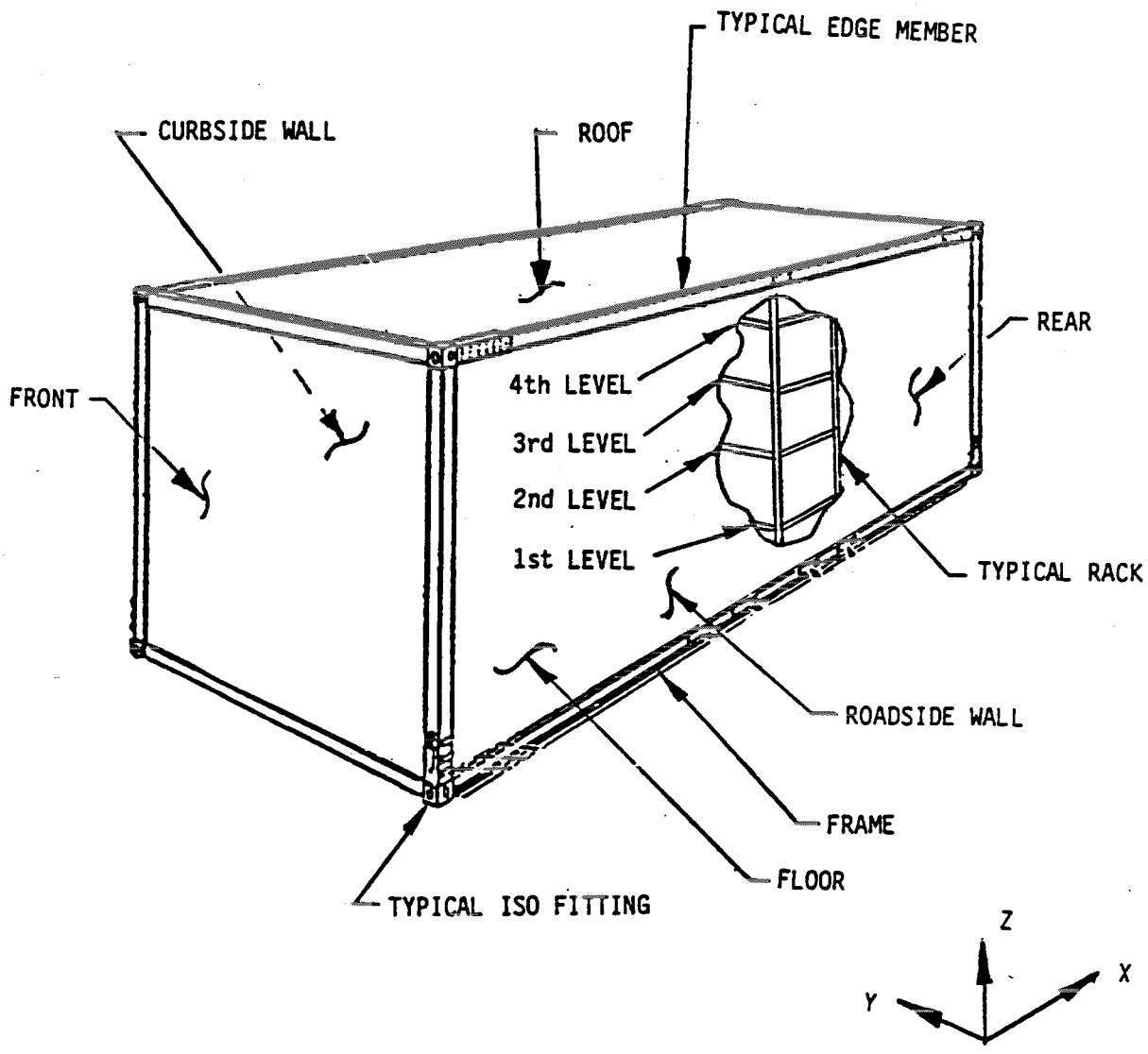

FIGURE 4

ISO 20' SHELTER

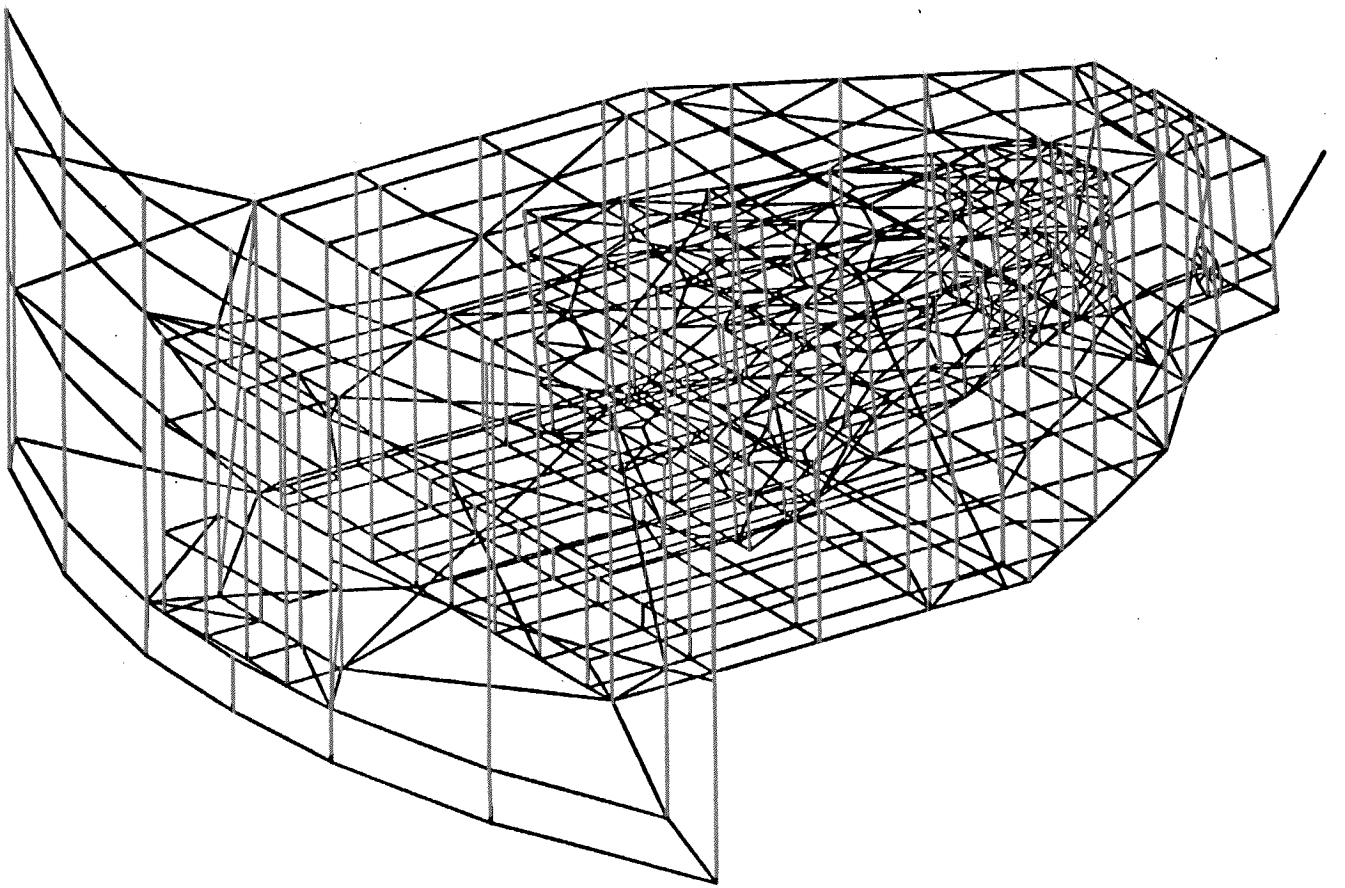

FIGURE 5

WFPC FINITE ELEMENT MODEL

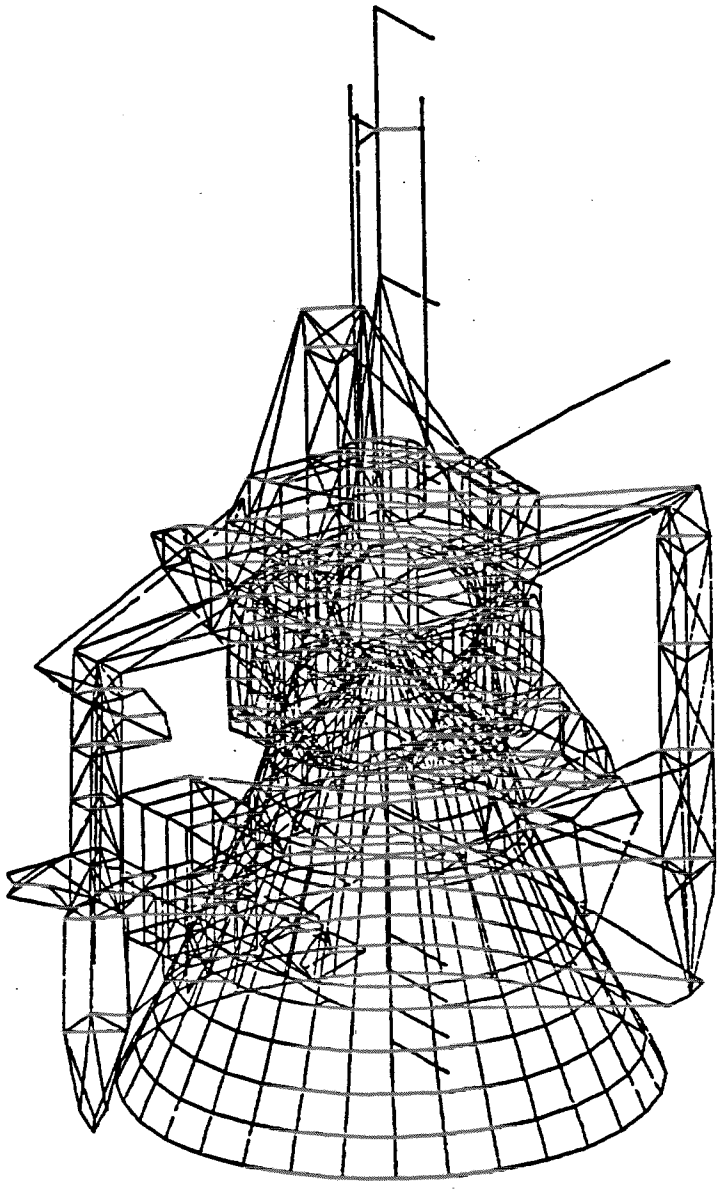

FIGURE 6

GLL FINITE ELEMENT MODEL

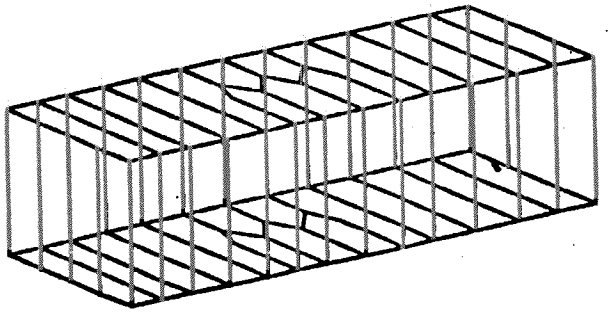

SHELTER HOOPS, END VERTICALS AND EDGES

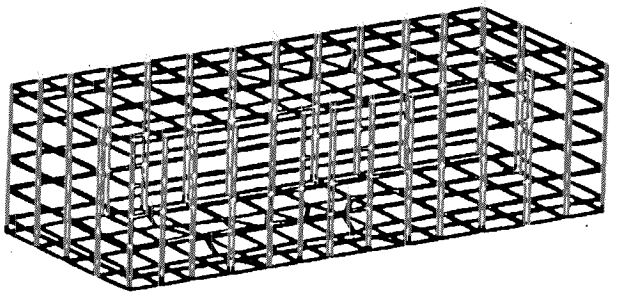

SHELTER WALLS, ROOF, FLOOR AND ENDS

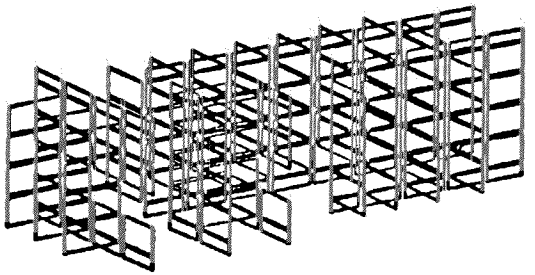

RACK AND WORK STATION FACES, BACKS, SIDES AND INNER DOOR

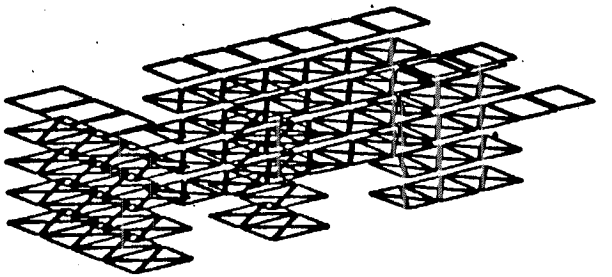

RACK AND WORK STATION EQUIPMENT, SHELVES AND CLOSEOUTS

FIGURE 7

FINITE ELEMENT MODEL, ISO 20' SHELTER

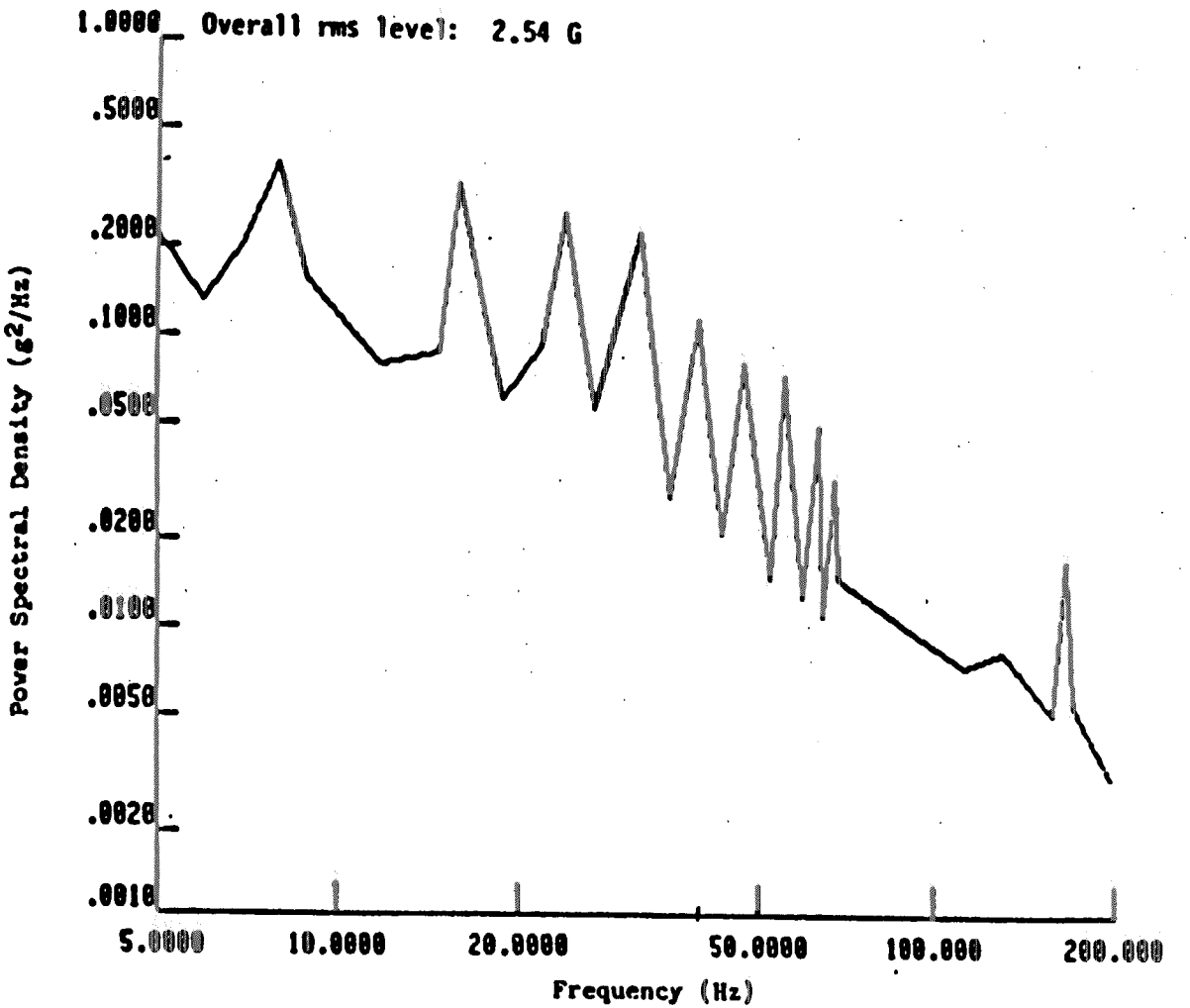

BREAKPOINTS FREQ	PSD VALUE
5	.22130
6	.13140
7	.20540
8	.38230
9	.15630
12	.07990
15	.08830
16	.32940
19	.06000
22	.09280
24	.26340
27	.05640
32	.22690
36	.02820
40	.11600
44	.02090
48	.08190
53	.01480
56	.07420
60	.01270
64	.04980
65	.01100
68	.03260
69	.01480
114	.00740
132	.00830
160	.00510
169	.01710
173	.00550
200	.00310

FIGURE 8

BASIC TRANSPORTATION, COMPOSITE TACTICAL WHEELED ENVIRONMENT, LONGITUDINAL AXIS (X)

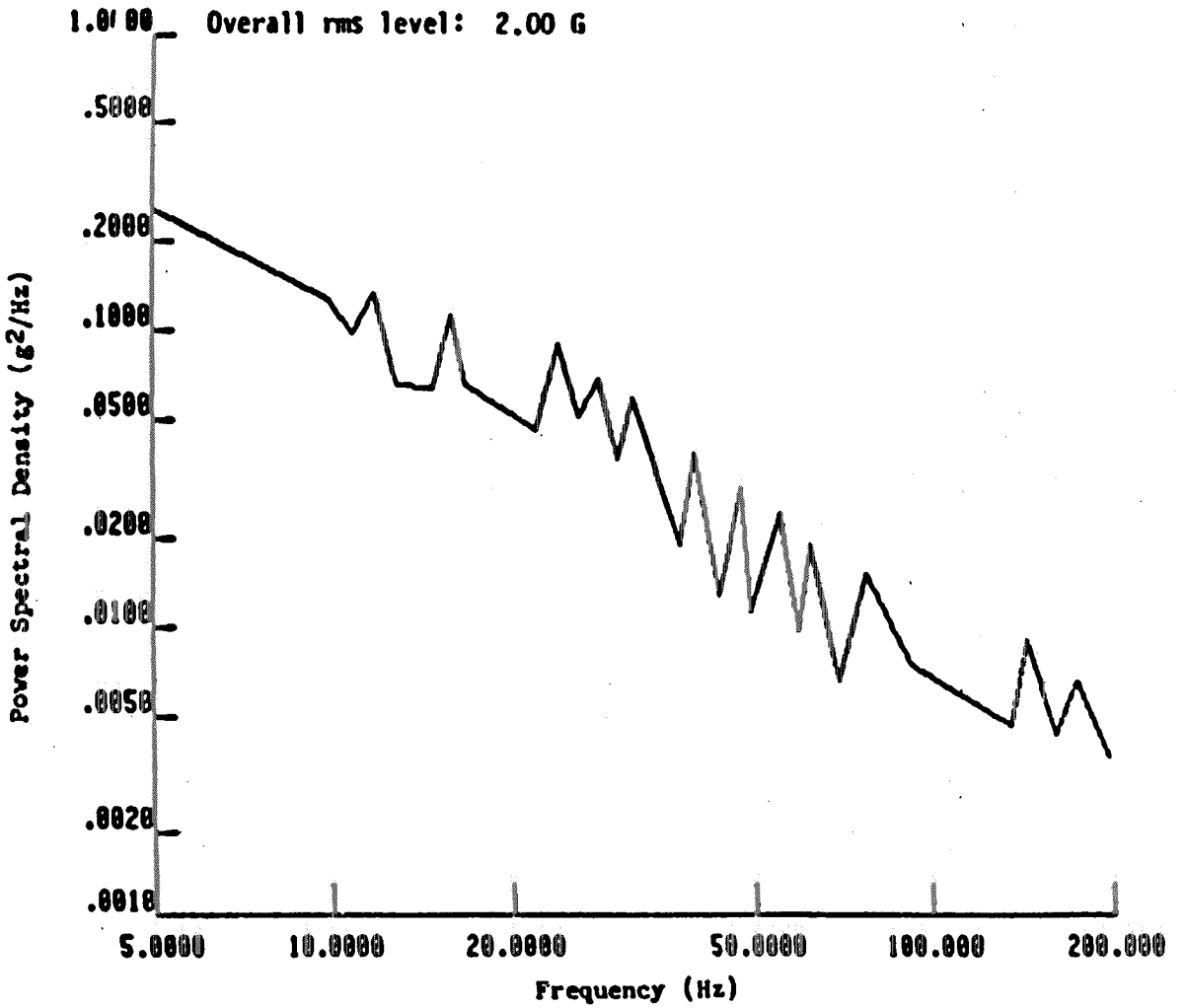

BREAKPOINTS

FREQ	PSD VALUE
5	.25490
10	.13030
11	.09670
12	.13360
13	.06500
15	.06340
16	.11230
17	.06500
22	.04590
24	.08980
26	.05070
28	.06630
30	.03670
32	.05080
38	.01920
40	.03860
44	.01290
48	.02940
50	.01140
56	.02460
60	.00960
63	.01880
70	.00660
78	.01500
93	.00730
137	.00460
145	.00910
162	.00430
176	.00660
200	.00360

FIGURE 9

BASIC TRANSPORTATION, COMPOSITE TACTICAL WHEELED ENVIRONMENT, TRANSVERSE AXIS (Y)

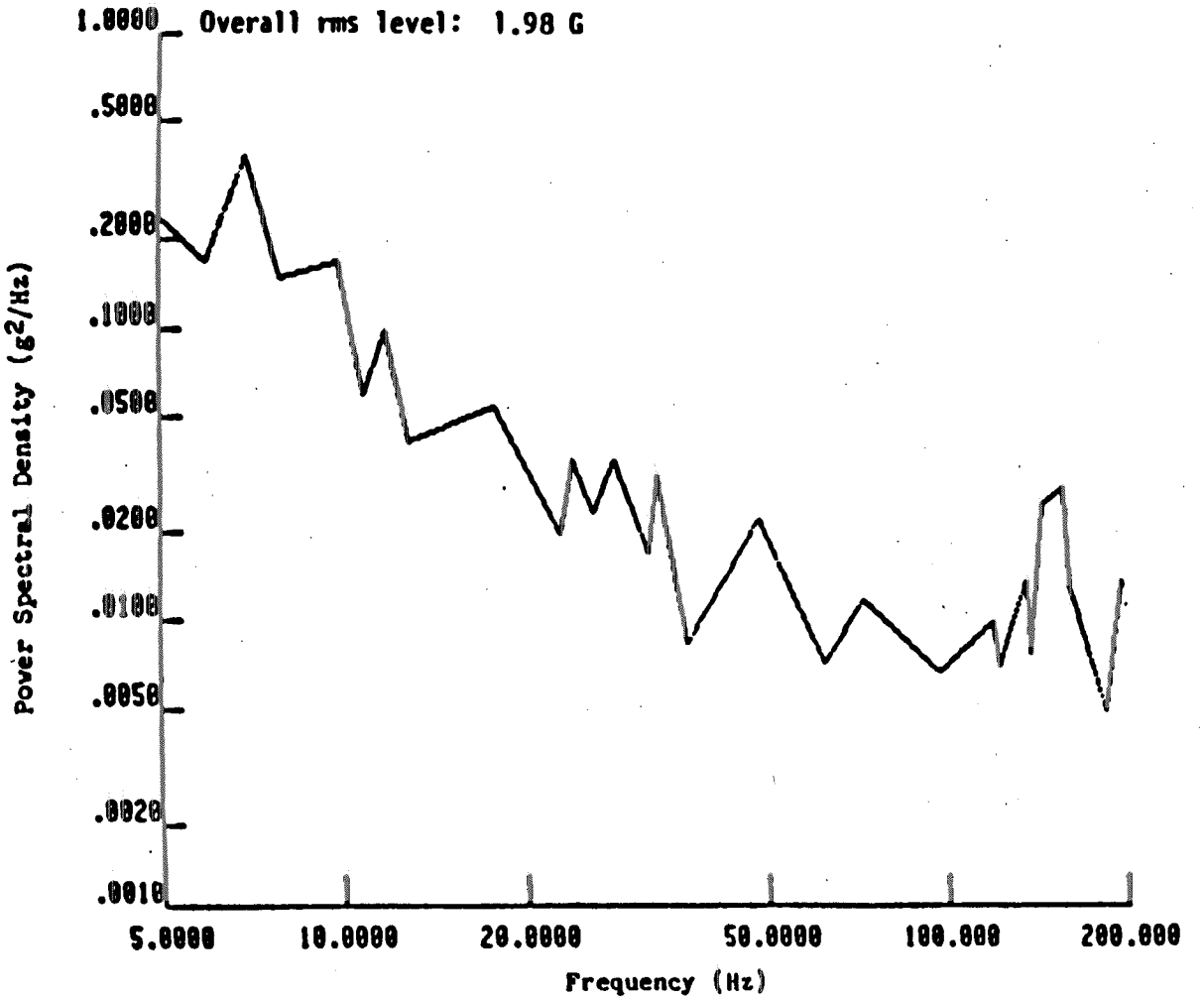

BREAKPOINTS

FREQ	PSD VALUE
5	.23040
6	.16040
7	.38230
8	.14870
10	.16840
11	.05930
12	.09750
13	.04090
18	.05370
23	.01940
24	.03520
26	.02310
28	.03520
32	.01670
33	.03110
37	.00810
49	.02190
63	.00700
73	.01150
98	.00666
120	.00970
123	.00680
130	.01340
140	.00760
146	.02490
159	.02820
163	.01300
188	.00480
200	.01340

FIGURE 10

BASIC TRANSPORTATION, COMPOSITE TACTICAL WHEELED ENVIRONMENT, VERTICAL AXIS (Z)

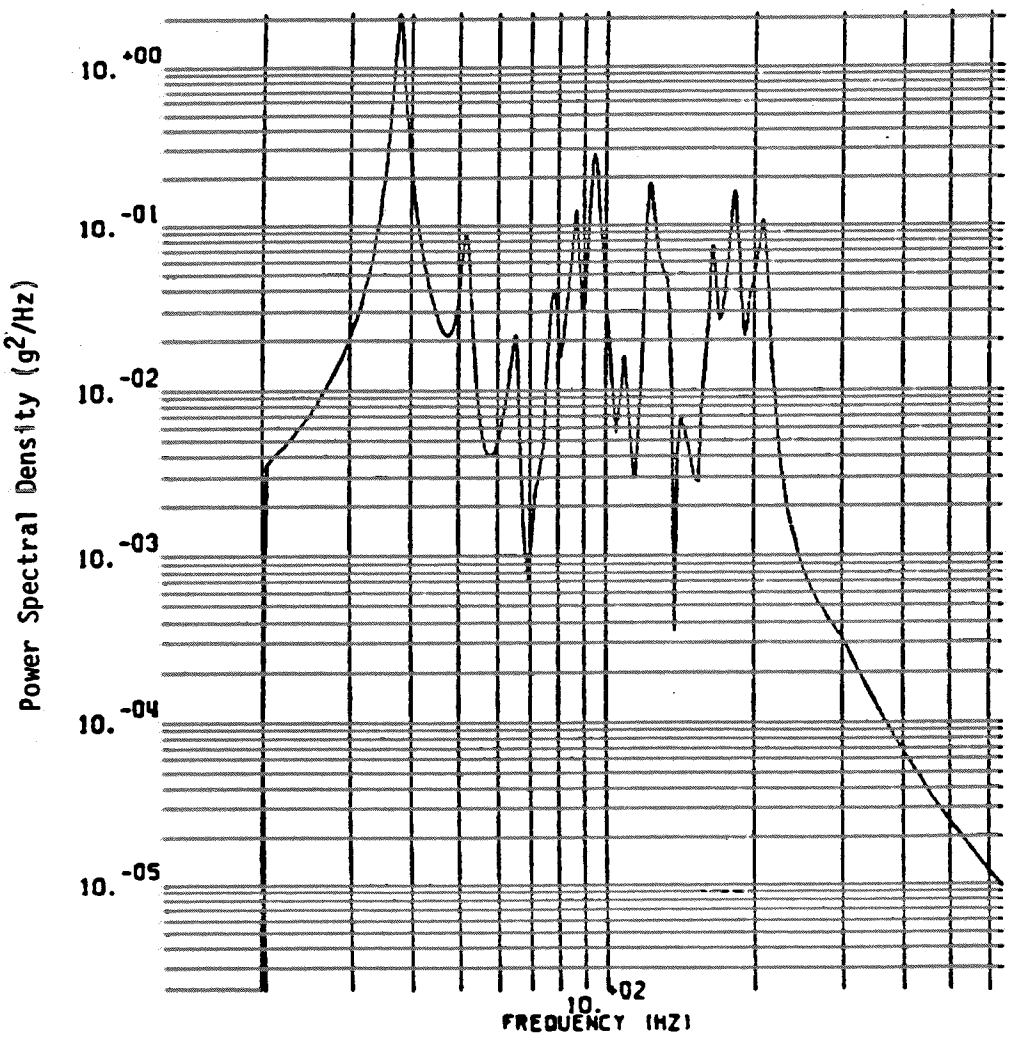

FIGURE 11

WFPC RANDOM VIBRATION, RADIATOR CORNER, VI DIRECTION

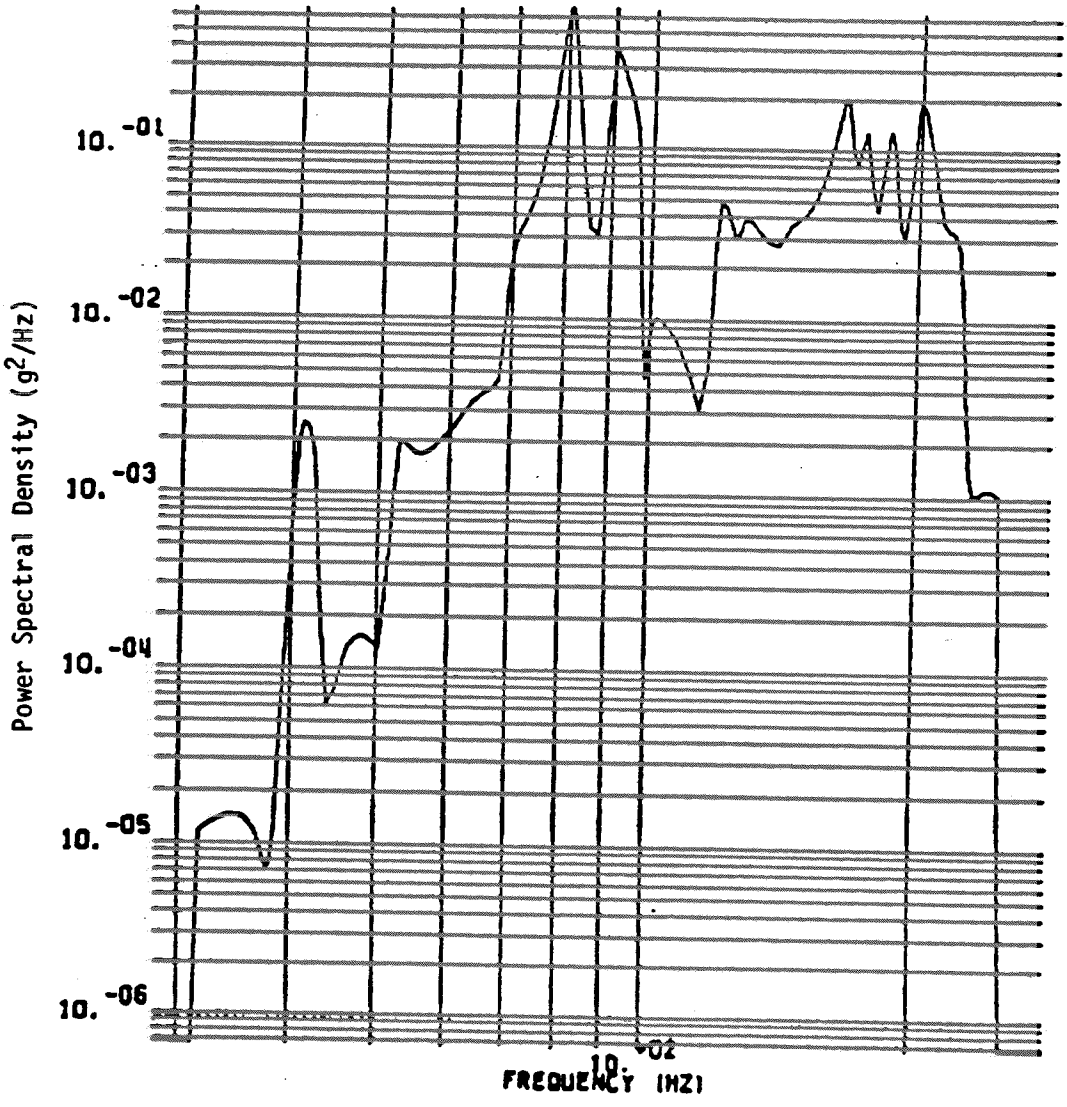

FIGURE 12

WFPC ACOUSTIC RESPONSE,
RADIATOR CORNER, VI DIRECTION

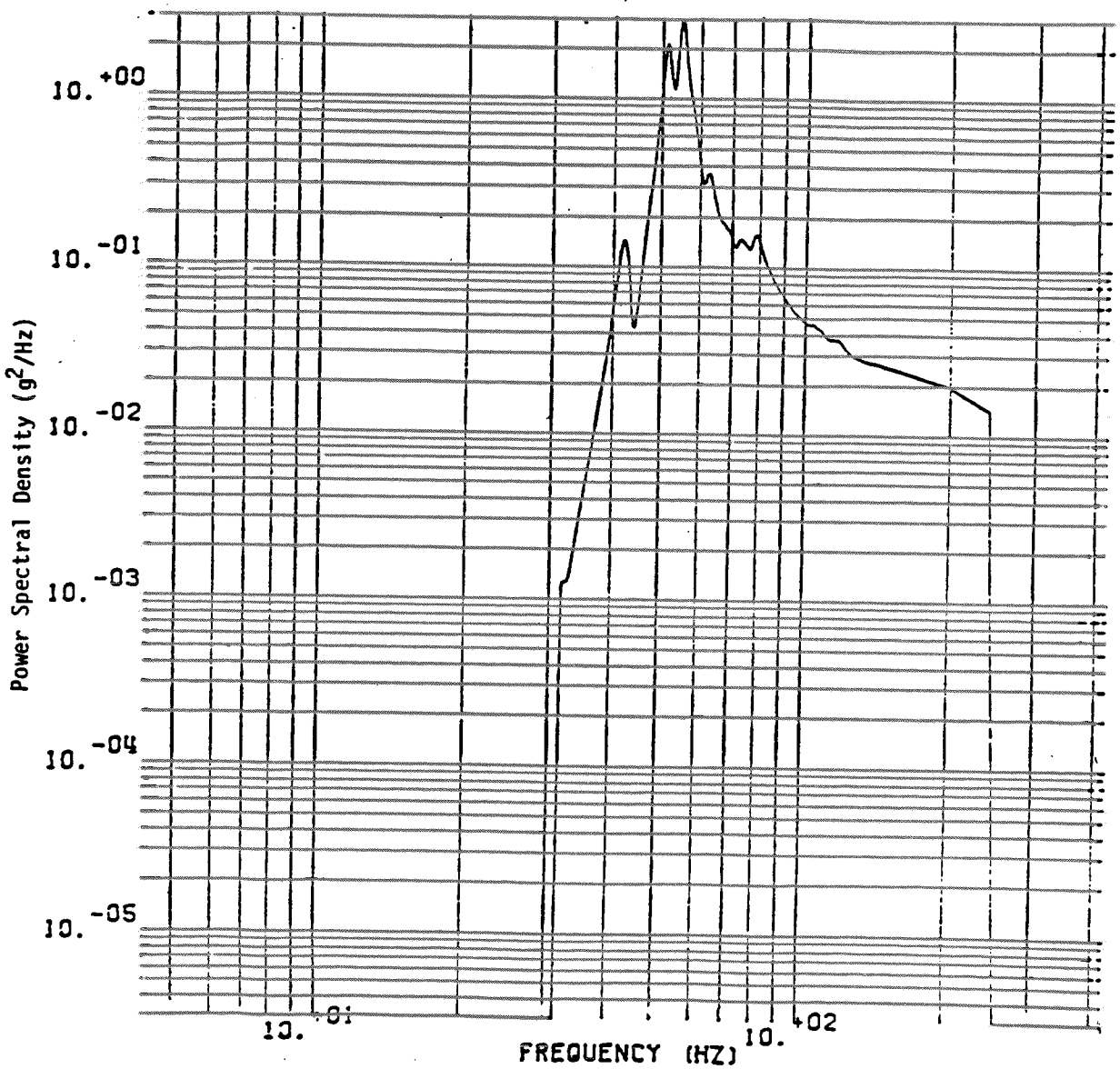

FIGURE 13

GLL ACOUSTIC RESPONSE, SXA C.G.,

X DIRECTION

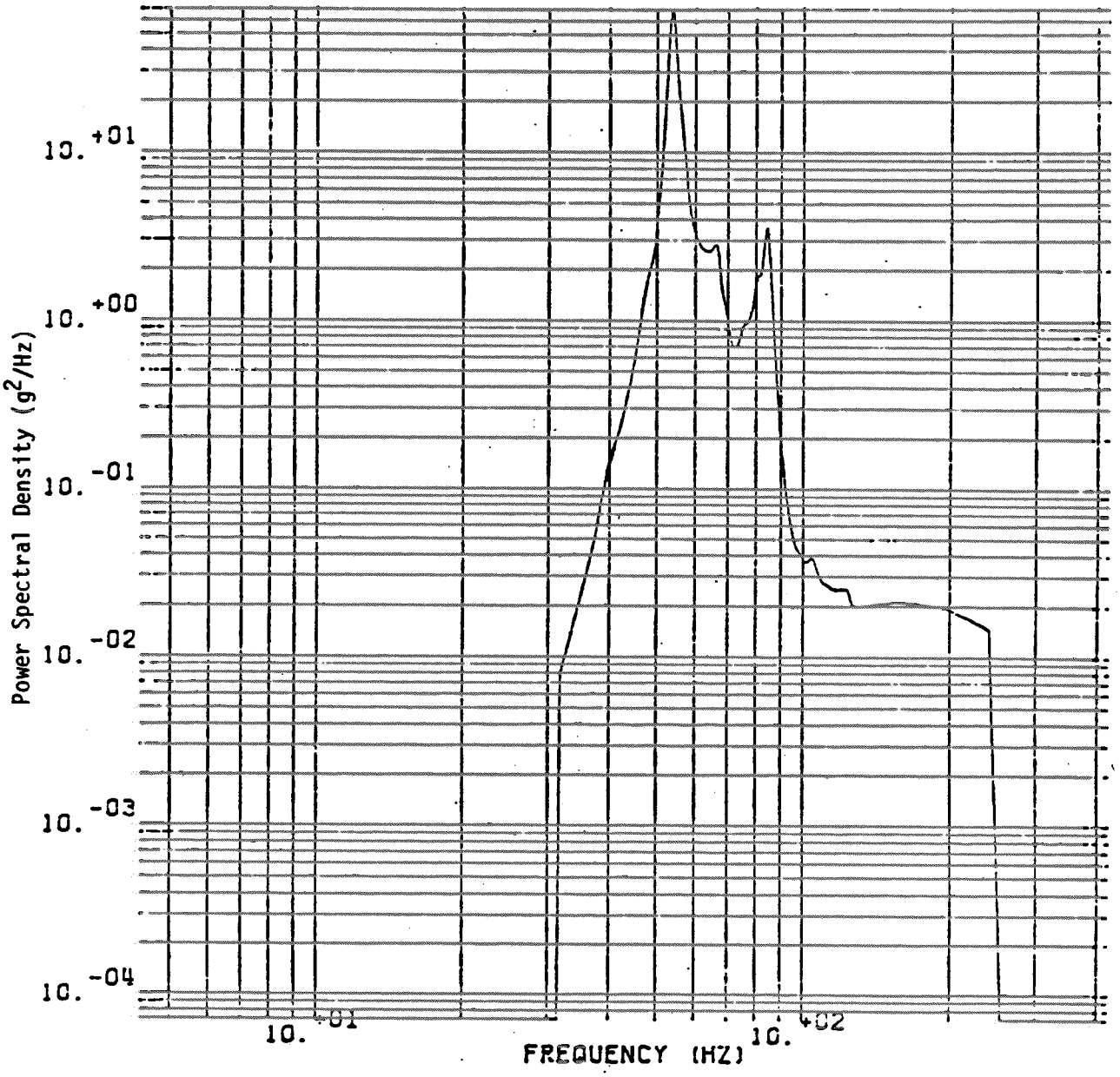

FIGURE 14

GLL ACOUSTIC RESPONSE, DESPUN BOX,
ANTENNA SIDE, X DIRECTION

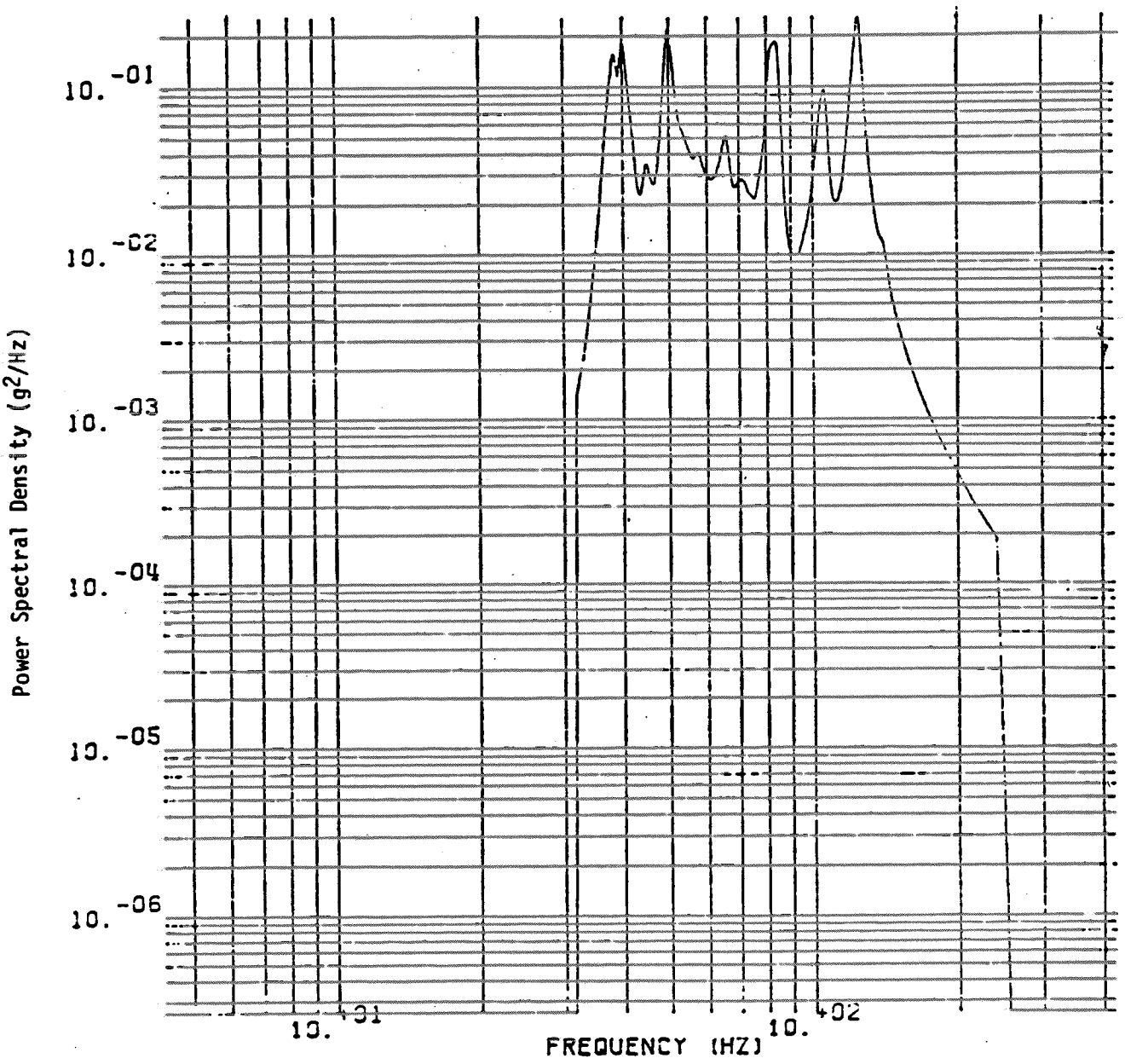

FIGURE 15

GLL ACOUSTIC RESPONSE, SCIENCE

BOOM MAGNETOMETER, Y DIRECTION

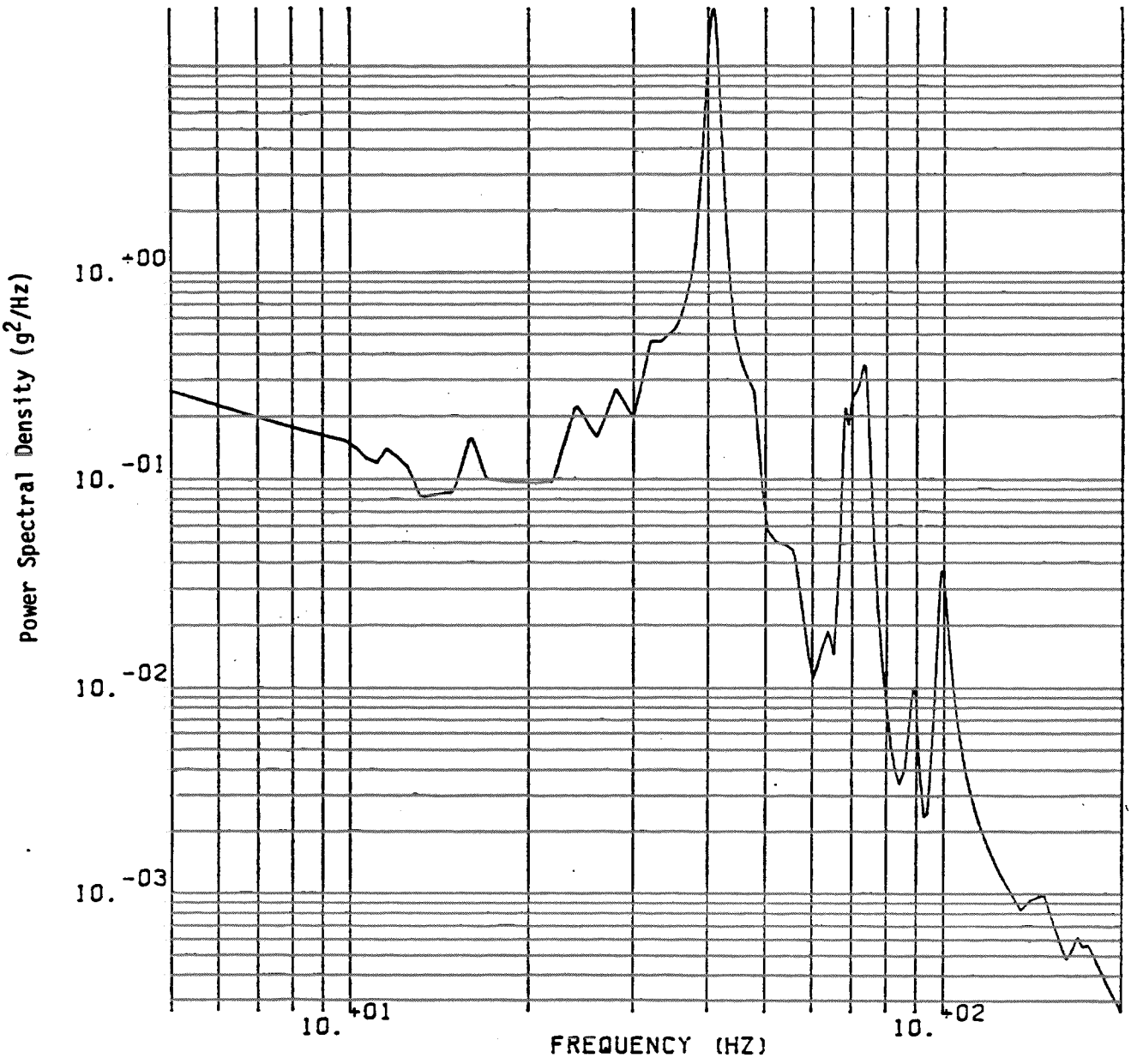

FIGURE 16

WORK STATION EQUIPMENT RANDOM VIBRATION RESPONSE,
ROADSIDE, 4th LEVEL, Y DIRECTION

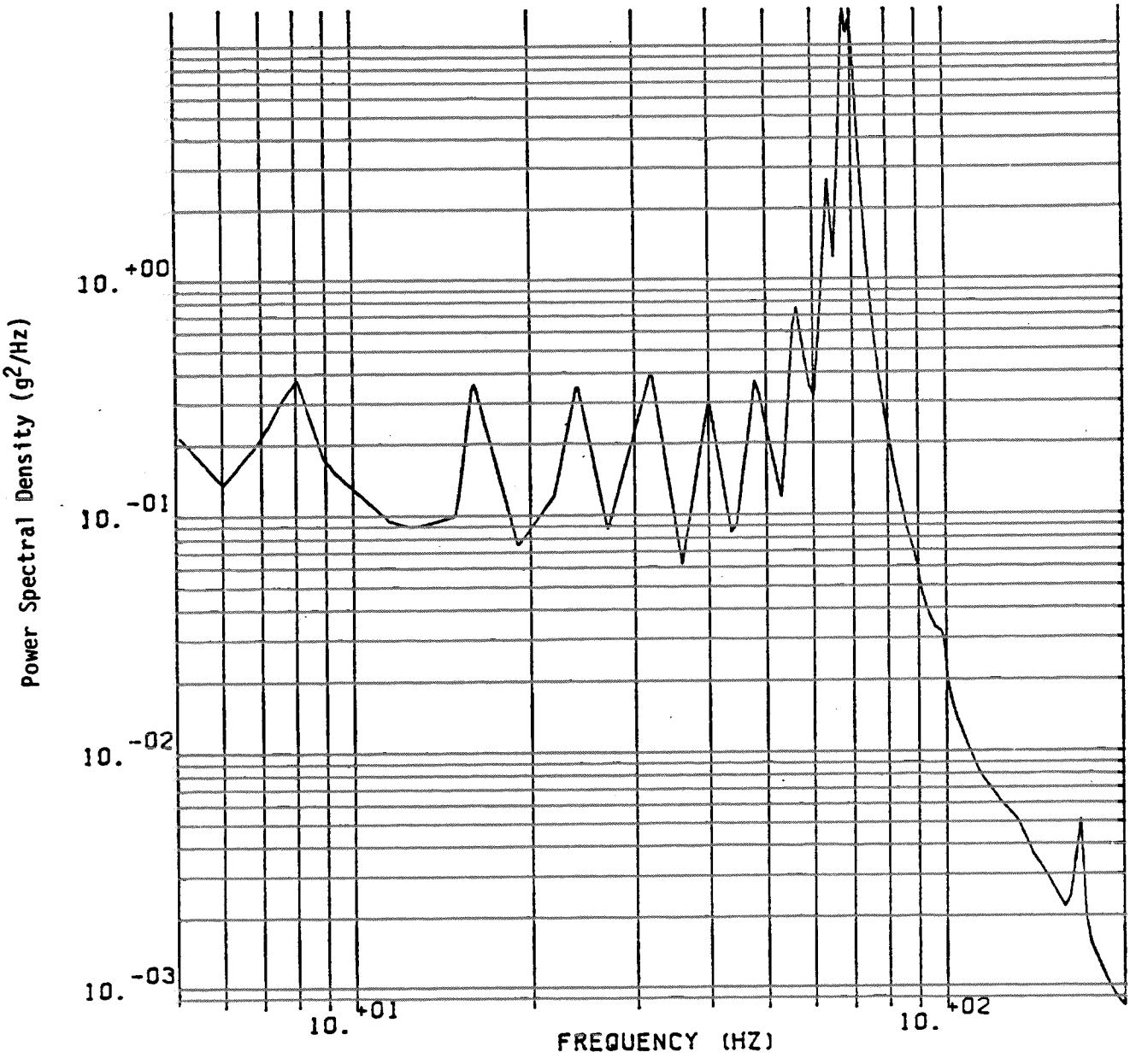

FIGURE 17

RACKED EQUIPMENT RANDOM VIBRATION RESPONSE,
CURBSIDE, 4th LEVEL, X DIRECTION

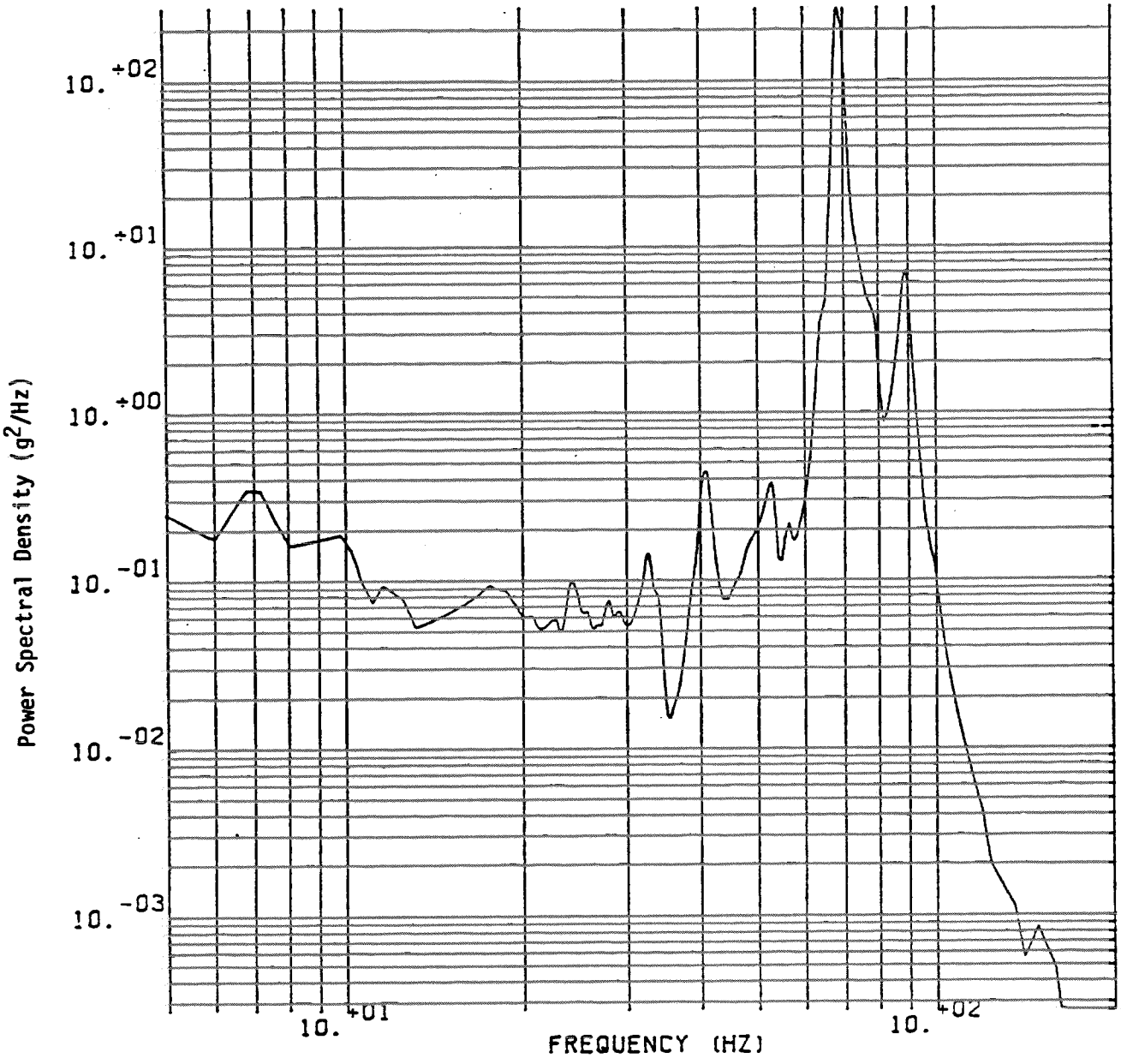

FIGURE 18

RACKED EQUIPMENT RANDOM VIBRATION RESPONSE,
ROADSIDE, 3rd LEVEL, Z DIRECTION

APPENDIX A

FUNDAMENTAL AND LOW ORDER NORMAL MODE ANALYSIS TO DETERMINE THE CROSS-POWER SPECTRUM AND VARIANCE OF THE RESPONSE*

By separation of variables , the dynamic response of a structure can be described by a set of characteristic functions $\{\varphi^n\}$ and generalized coordinates $q_n(t)$ where the response $y(v_i, t)$ at point v_i on the structure relative to the base motion coordinate $x(t)$ is (Reference 1)

$$y(v_i, t) = \sum \varphi_n(v_i) q_n(t) \tag{1-1}$$

The absolute response $z(v_i, t)$ is therefore defined as

$$z(v_i, t) = x(t) + y(v_i, t)$$

or

$$z(v_i, t) = x(t) + \sum \varphi_n (v_i)\, q_n(t)$$

Since stress in a structural element (e_i) is directly proportional to relative displacement, it too can be expressed directly in terms of a stress modal characteristic function $\{\psi^n\}$

$$M (e_i, t) = \sum \psi_n(e_i) q_n(t) \tag{1-2}$$

For small viscous damping, the equation of motion of the n^{th} generalized coordinate is

$$\ddot{q}_n (t) + 2 \zeta_n \omega_n \dot{q}_n (t) + \omega_n^2 q_n (t) = \frac{F_n(t)}{M_n} \tag{1-3}$$

Where ω_n is the n^{th} natural frequency or characteristic value in radians per second and ζ_n is the viscous modal critical damping ratio

*This material was developed by Michael D. Lamers and is found in "Structural Dynamic Random Response Analysis", MRI-TR-8036, dated September, 1971.

where $H_n(j\omega)$ is the complex frequency response function (forced motion transfer function). For a system with viscous damping we have

$$H_n(j\omega) = \left[1 - (\omega/\omega_n)^2 + j2\zeta_n\, \omega/\omega_n\right]^{-1} \tag{1-6}$$

For structural damping

$$H_n(j\omega) = \left[1 - (\omega/\omega_n)^2 + js_n\right]^{-1} \tag{1-7}$$

For a stationary stochastic process, the expected value of the product

$$E\left\{Q_n(j\omega) \cdot Q_m{}^*(j\omega)\right\} = S_{q_n q_m}(j\omega) \tag{1-8}$$

where

$E\{\ \}$ denotes expected value

$*$ denotes complex conjugate

and

$S_{q_n q_m}(j\omega)$ is the two sided cross power spectrum between q_n and q_m.

Combining Equations 1-5 and 1-8 gives

$$S_{q_n q_m}(j\omega) = E\left\{\frac{H_n(j\omega)\,H_m^*(j\omega)}{\omega_n^2\omega_m^2 M_n M_m}\int_0^v\int_0^{v'}\varphi_n(v)\varphi_m(v')F(v,j\omega)F^*(v',j\omega)dvdv'\right\} \quad (1\text{-}9)$$

Since $F(v,j\omega)$ and $F^*(v',j\omega)$ are the only random variables, Equation 1-9 can be written as

$$S_{q_n q_m}(j\omega) = \frac{H_n(j\omega)H_m^*(j\omega)}{\omega_n^2\omega_m^2 M_n M_m}\int_0^v\int_0^{v'}\varphi_n(v)\varphi_m(v')E\left\{F(v,j\omega)F^*(v',j\omega)\right\}dvdv' \quad (1\text{-}10)$$

As in Equation 1-8, we have

$$E\left\{F(v,j\omega)\,F^*(v',j\omega)\right\} = S_{f_v f_{v'}}(j\omega) \quad (1\text{-}11)$$

where $S_{f_v f_{v'}}(j\omega)$ is the two sided cross-power spectrum of the forcing function between v and v'.

For a real causal process we have

$$G_{xy}(j\omega) = \begin{cases} 2\,S_{xy}(j\omega) & \omega > 0 \\ 0 & \omega < 0 \end{cases} \quad (1\text{-}12)$$

where $G_{xy}(j\omega)$ is the one sided cross-power spectrum between x and y.

Combining Equations 1-10, 1-11 and 1-12 gives

$$G_{q_n q_m}(j\omega) = \frac{H_n(j\omega)H^*_m(j\omega)}{\omega_n^2\omega_m^2 M_n M_m}\int_0^v\int_0^{v'}\varphi_n(v)\varphi_m(v')G_{f_v f_{v'}}(j\omega)dvdv' \quad (1\text{-}13)$$

where the double integral is called the generalized forcing cross-power spectrum and is defined as

$$G_{f_n f_m}(j\omega) = \int_0^v \int_0^{v'} \varphi_n(v)\varphi_m(v') G_{f_v f_{v'}}(j\omega)\,dv\,dv' \tag{1-14}$$

Equation 1-13 and 1-14 can be written in general form as

$$G_{q_n q_m}(j\omega) = \frac{H_n(j\omega)\, H_m^*(j\omega)}{\omega_n^2 \omega_m^2 M_n M_m} G_{f_n f_m}(j\omega) \tag{1-15}$$

When the forcing cross power spectrum is real and separable in space and time (or frequency) it can be expressed as

$$G_{f_v f_{v'}}(\omega) = \mathrm{PSD}(\omega)\, \mathcal{F}(v,v') \tag{1-16}$$

where $\mathcal{F}(v,v')$ is the non frequency dependent normalized real forcing cross power spectrum between point v and v'. $\mathcal{F}(v,v')$ can be further expressed in terms of the coherence function ($C_{vv'}$) between v and v' and the normalized forcing power coefficient (P_v) at the point v and v' of the structure as:

$$\mathcal{F}(v,v') \triangleq \left[P_v\ P_{v'}\right]^{\frac{1}{2}} C_{vv'} \tag{1-17}$$

where the product of $\mathrm{PSD}(\omega)P_v$ has dimensions of $(\text{Force})^2$ per unit bandwidth or $(\text{Torque})^2$ per unit bandwidth. $C_{vv'}$ is a real dimensionless quantity where

$$0 \leq C_{vv'} \leq 1$$

Equation 1-14 can therefore be expressed as:

$$G_{f_n f_m}(\omega) = PSD(\omega) \int_0^V \int_0^{V'} \varphi_n(v)\varphi_m(v') \left[P_v P_{v'}\right]^{\frac{1}{2}} C_{vv'}\,dvdv' \qquad (1\text{-}18)$$

The double integral in Equation 1-18 is sometimes referred to as the generalized cross-mode forcing power spectrum participation factor and is denoted by

$$\Gamma_{nm} = \int_0^V \int_0^{V'} \varphi_n(v)\varphi_m(v') \left[P_v P_{v'}\right]^{\frac{1}{2}} C_{vv'}\,dvdv'$$

To find the point response, we take the expected value of the Fourier Transform of $y(v_i,t)$ as shown in Equation 1-1.

$$E\left\{y(v_i,\omega)\; y^*(v_i,\omega)\right\} = E\left\{\sum\sum \varphi_n(v_i)\varphi_m(v_i) Q_n(j\omega) Q_m^*(j\omega)\right\} \qquad (1\text{-}19)$$

Combining Equations 1-8, 1-12 and 1-19 gives

$$G^y_{v_i v_j}(j\omega) = \sum_n \sum_m \varphi_n(v_i)\varphi_m(v_j) G_{q_n q_m}(j\omega) \qquad (1\text{-}20)$$

Equation 1-20 is the general expression for the complex cross-power spectrum response between point i and j on the structure. If i equals j we get the point response power spectral density which is a positive real quantity

$$G^{y}_{v_i}(\omega) = \sum_{n}\sum_{m} \varphi_n(v_i)\varphi_m(v_i)G_{q_n q_m}(j\omega) \tag{1-21}$$

or for computation purposes this can be written as

$$G^{y}_{v_i}(\omega) = \sum_{n}\sum_{m} \varphi_n(v_i)\varphi_m(v_i)\ \mathrm{Re}\left[G_{q_n q_m}(j\omega)\right] \tag{1-21-a}$$

where $\mathrm{Re}\left[\ A\ \right]$ denotes the real part of A.

Combining Equations 1-15, 1-18 and 1-21 gives the expression for the spatial point relative response power spectral density at point v_i

$$G^{y}_{v_i}(\omega)=\sum_{n}\sum_{m} \varphi_n(v_i)\varphi_m(v_i)\left\{\frac{H_n(j\omega)H^{*}_m(j\omega)}{\omega_n^2\omega_m^2 M_n M_m}\ \mathrm{PSD}(\omega)\int_{o}^{v}\int_{o}^{v'}\varphi_n(v)\varphi_m(v')\left[P_v P_{v'}\right]^{\frac{1}{2}}C_{vv'}\,dvdv'\right\} \tag{1-22}$$

Combining Equations 1-15, 1-18 and 1-20 gives the expression for the complex cross-power spectrum between point v_i and v_j

$$G^{y}_{v_i v_j}(j\omega)=\sum_{n}\sum_{m} \varphi_n(v_i)\varphi_m(v_j)\left\{\frac{H_n(j\omega)H^{*}_m(j\omega)}{\omega_n^2\omega_m^2 M_n M_m}\ \mathrm{PSD}(\omega)\int_{o}^{v}\int_{o}^{v'}\varphi_n(v)\varphi_m(v')\left[P_v P_{v'}\right]^{\frac{1}{2}}C_{vv'}\,dvdv'\right\} \tag{1-23}$$

The absolute response power spectral density, $G^{z}_{v_i}(\omega)$, for a base motion excitation, $G^{x}(\omega) = PSD^{x}(\omega)$, can be expressed in terms of the relative response power spectral density and the forced motion transfer function by the following expression

$$G^{z}_{v_i}(\omega) = G^{y}_{v_i}(\omega) + PSD_x(\omega)\left\{1 + 2\sum_{n=1} \frac{\varphi_n(v_i)\,\Gamma_{nn}}{\omega_n^2\, M_n} \mathrm{Re}\left[H_n(j\omega)\right]\right\} \qquad (1\text{-}24)$$

The variance or mean square response at point v_i is given by

$$\sigma^2_y(v_i) = \int_0^\infty G^{y}_{v_i}(\omega)\, d\omega \qquad (1\text{-}25)$$

$$= \sum_n \sum_m \varphi_n(v_i)\varphi_m(v_i) \int_0^\infty \mathrm{Re}\left[G_{q_n q_m}(j\omega)\right] d\omega \qquad (1\text{-}25\text{-a})$$

The integral term in Equation (1-25-a) is equivalent to the real portion (contribution) of the covariance between $q_n(t)$ and $q_m(t)$ which is equal to the cross correlation coefficient with zero delay, $R_{q_n q_m}(0)$. This will be expressed as follows:

$$\int_0^\infty \mathrm{Re}\left[G_{q_n q_m}(j\omega)\right] d\omega = E\left\{q_n(t) q_m^{*}(t)\right\} = R_{q_n q_m}(0) \qquad (1\text{-}26)$$

combining Equations (1-25-a) and (1-26) gives

$$\sigma^2_y(v_i) = \sum_n \sum_m \varphi_n(v_i)\, \varphi_m(v_i)\, R_{q_n q_m}(0) \qquad (1\text{-}27)$$

It should be noted that $R_{q_n q_m}(0)$ can be a negative value for $n \neq m$. The following relation, known as Schwarz inequality, can be shown:

$$\left| R_{q_n q_m}(0) \right| \leq \left[R_{q_n q_n}(0)\, R_{q_m q_m}(0)\right]^{\frac{1}{2}} \qquad (1\text{-}28)$$

The variance or mean square stress in an element (e_i) can be solved similar to Equation (1-22), using Equation (1-2) giving

$$\sigma_M^2 (e_i) = \sum_n \sum_m \psi_n(e_i)\psi_m(e_i) R_{q_n q_m}(0) \qquad (1\text{-}29)$$

Equations (1-22), (1-23), (1-27) and (1-29) are the basic equations used.